

Master's thesis in
Applied Computer Science

CoolingGen

A parametric 3D-modeling software for turbine
blade cooling geometries using NURBS

August 25, 2022

Institute for Numerical and Applied Mathematics
at the Georg-August-University Göttingen

Institute for Propulsion Technology at the
German Aerospace Center in Göttingen

Bachelor's and master's theses at the Center for
Computational Sciences at the
Georg-August-University Göttingen

Julian Lüken
`julian.lueken@dlr.de`

Georg-August-University Göttingen
Institute of Computer Science

☎ +49 (551) 39-172000

☎ +49 (551) 39-14403

✉ office@cs.uni-goettingen.de

www.informatik.uni-goettingen.de

I hereby declare that this thesis has been written by myself and no other resources than those mentioned have been used.

A handwritten signature in blue ink, appearing to read 'Lüken', with a stylized, cursive script.

Göttingen, August 25, 2022

Abstract

Lorem ipsum dolor sit amet, consectetur adipiscing elit. Ut purus elit, vestibulum ut, placerat ac, adipiscing vitae, felis. Curabitur dictum gravida mauris. Nam arcu libero, nonummy eget, consectetur id, vulputate a, magna. Donec vehicula augue eu neque. Pellentesque habitant morbi tristique senectus et netus et malesuada fames ac turpis egestas. Mauris ut leo. Cras viverra metus rhoncus sem. Nulla et lectus vestibulum urna fringilla ultrices. Phasellus eu tellus sit amet tortor gravida placerat. Integer sapien est, iaculis in, pretium quis, viverra ac, nunc. Praesent eget sem vel leo ultrices bibendum. Aenean faucibus. Morbi dolor nulla, malesuada eu, pulvinar at, mollis ac, nulla. Curabitur auctor semper nulla. Donec varius orci eget risus. Duis nibh mi, congue eu, accumsan eleifend, sagittis quis, diam. Duis eget orci sit amet orci dignissim rutrum.

Nam dui ligula, fringilla a, euismod sodales, sollicitudin vel, wisi. Morbi auctor lorem non justo. Nam lacus libero, pretium at, lobortis vitae, ultricies et, tellus. Donec aliquet, tortor sed accumsan bibendum, erat ligula aliquet magna, vitae ornare odio metus a mi. Morbi ac orci et nisl hendrerit mollis. Suspendisse ut massa. Cras nec ante. Pellentesque a nulla. Cum sociis natoque penatibus et magnis dis parturient montes, nascetur ridiculus mus. Aliquam tincidunt urna. Nulla ullamcorper vestibulum turpis. Pellentesque cursus luctus mauris.

Nulla malesuada porttitor diam. Donec felis erat, congue non, volutpat at, tincidunt tristique, libero. Vivamus viverra fermentum felis. Donec nonummy pellentesque ante. Phasellus adipiscing semper elit. Proin fermentum massa ac quam. Sed diam turpis, molestie vitae, placerat a, molestie nec, leo. Maecenas lacinia. Nam ipsum ligula, eleifend at, accumsan nec, suscipit a, ipsum. Morbi blandit ligula feugiat magna. Nunc eleifend consequat lorem. Sed lacinia nulla vitae enim. Pellentesque tincidunt purus vel magna. Integer non enim. Praesent euismod nunc eu purus. Donec bibendum quam in tellus. Nullam cursus pulvinar lectus. Donec et mi. Nam vulputate metus eu enim. Vestibulum pellentesque felis eu massa.

Zusammenfassung

Quisque ullamcorper placerat ipsum. Cras nibh. Morbi vel justo vitae lacus tincidunt ultrices. Lorem ipsum dolor sit amet, consectetur adipiscing elit. In hac habitasse platea dictumst. Integer tempus convallis augue. Etiam facilisis. Nunc elementum fermentum wisi. Aenean placerat. Ut imperdiet, enim sed gravida sollicitudin, felis odio placerat quam, ac pulvinar elit purus eget enim. Nunc vitae tortor. Proin tempus nibh sit amet nisl. Vivamus quis tortor vitae risus porta vehicula.

Fusce mauris. Vestibulum luctus nibh at lectus. Sed bibendum, nulla a faucibus semper, leo velit ultricies tellus, ac venenatis arcu wisi vel nisl. Vestibulum diam. Aliquam pellentesque, augue quis sagittis posuere, turpis lacus congue quam, in hendrerit risus eros eget felis. Maecenas eget erat in sapien mattis porttitor. Vestibulum porttitor. Nulla facilisi. Sed a turpis eu lacus commodo facilisis. Morbi fringilla, wisi in dignissim interdum, justo lectus sagittis dui, et vehicula libero dui cursus dui. Mauris tempor ligula sed lacus. Duis cursus enim ut augue. Cras ac magna. Cras nulla. Nulla egestas. Curabitur a leo. Quisque egestas wisi eget nunc. Nam feugiat lacus vel est. Curabitur consectetur.

Suspendisse vel felis. Ut lorem lorem, interdum eu, tincidunt sit amet, laoreet vitae, arcu. Aenean faucibus pede eu ante. Praesent enim elit, rutrum at, molestie non, nonummy vel, nisl. Ut lectus eros, malesuada sit amet, fermentum eu, sodales cursus, magna. Donec eu purus. Quisque vehicula, urna sed ultricies auctor, pede lorem egestas dui, et convallis elit erat sed nulla. Donec luctus. Curabitur et nunc. Aliquam dolor odio, commodo pretium, ultricies non, pharetra in, velit. Integer arcu est, nonummy in, fermentum faucibus, egestas vel, odio.

Contents

1	Introduction	1
1.1	Motivation	1
1.2	State of the Art	1
1.3	Problem Statement	1
2	Methods	2
2.1	Bézier Curves	2
2.1.1	Definition	2
2.1.2	De Casteljau's Algorithm	3
2.1.3	Properties	4
2.2	Non-Uniform Rational B-splines (NURBS)	5
2.2.1	Definition	5
2.2.2	De Boor's Algorithm	7
2.2.3	Properties	10
2.3	Methods on NURBS Objects	11
2.3.1	Point Inversion	11
2.3.2	Ray-Curve Intersection	13
2.3.3	Curve-Curve Intersection	16
2.3.4	Fillet Creation	16
2.4	Jet Engine Design Specifics	16
2.4.1	Fundamental Terms	16
2.4.2	The S2M Net	16
3	Results	17
3.1	Cooling Geometries And Their Parametrizations	17
3.1.1	Chambers	17
3.1.2	Turnarounds	17
3.1.3	Slots	17
3.1.4	Film Cooling Holes	17
3.1.5	Impingement Inserts	17
3.2	Export for CENTAUR	17
3.3	Export for Open CASCADE	17
4	Discussion	18
4.1	Future Work	18
4.2	Conclusion	18
5	References	19

1 Introduction

1.1 Motivation

1.2 State of the Art

1.3 Problem Statement

2 Methods

As stated before, Non-Uniform Rational B-splines (NURBS) curves and surfaces are used to model geometries in CoolingGen. In this chapter we will first introduce Bézier curves. We will then generalize Bézier curves to obtain B-spline curves and surfaces. Applying an embedding map and a projection map to B-spline curves and surfaces, we acquire NURBS curves and surfaces, which are a generalization of B-spline curves and surfaces. Furthermore, CoolingGen uses special geometric algorithms such as point inversion, curve intersection and curve fillet fitting, which we will also present.

2.1 Bézier Curves

Bézier curves are named after the French engineer Pierre Bézier, who famously utilized them in the 1960s to design car bodies for the automobile manufacturer Renault [Béz68]. Today, they are used in a wide variety of vector graphics applications (i.e. in font representation on computers). At first glance, the definition of the Bézier curve might seem cumbersome, but given the mathematical foundation and a few graphical representations, it becomes apparent why they are such a powerful tool in computer-aided design.

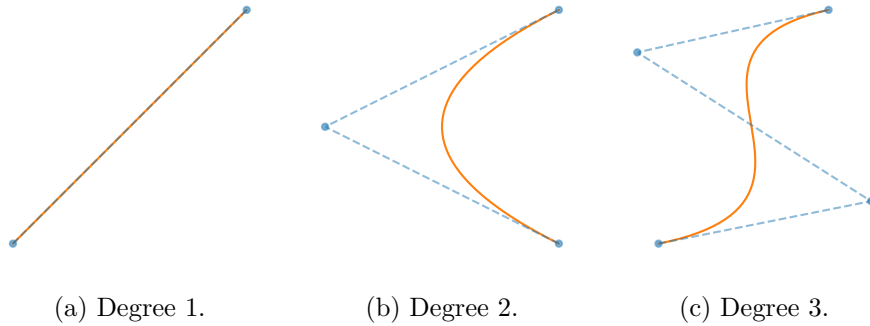


Figure 2.1: Bézier curves of different degrees (orange) and their control points (blue).

2.1.1 Definition

Definition 2.1.1. The *Bernstein basis polynomials* of degree n on the interval $[t_0, t_1]$ are defined as

$$b_{n,k,[t_0,t_1]}(t) := \frac{\binom{n}{k}(t_1 - t)^{n-k}(t - t_0)^k}{(t_1 - t_0)^n}, \quad (2.1)$$

for $k \in \{0, \dots, n\}$.

Definition 2.1.2. Let V a vector space. A *Bézier curve* of degree n is a parametric curve $B_{P,[t_0,t_1]} : [t_0, t_1] \rightarrow V$ that has a representation

$$B_{P,[t_0,t_1]}(t) = \sum_{k=0}^n b_{n,k,[t_0,t_1]}(t)P_k = \sum_{k=0}^n \frac{\binom{n}{k}(t_1 - t)^{n-k}(t - t_0)^k}{(t_1 - t_0)^n} P_k. \quad (2.2)$$

We call the elements of the set $P = \{P_0, P_1, \dots, P_n\} \subset V$ the *control points* of B_P .

Remark. Let $t_0 = 0$ and $t_1 = 1$. Then 2.2 simplifies to

$$b_{n,k}(t) := b_{n,k,[0,1]}(t) = \binom{n}{k} (1-t)^{n-k} t^k \quad (2.3)$$

and 2.1 simplifies to

$$B_P(t) := B_{P,[0,1]}(t) = \sum_{k=0}^n \binom{n}{k} (1-t)^{n-k} t^k P_k. \quad (2.4)$$

This case is the only case considered in this thesis. We also set the vector space V to be \mathbb{R}^3 unless specified otherwise.

2.1.2 De Casteljau's Algorithm

The computation of Equation 2.4 is usually performed using de Casteljau's algorithm. This is because the algorithm yields a simple implementation and lower complexity than straightforwardly computing Equation 2.4. The algorithm was proposed by Paul de Faget de Casteljau for the automobile manufacturer Citroën in the 1960s.

Algorithm 1 de Casteljau's algorithm

```

1: Input
2:    $P = \{P_0, P_1, \dots, P_n\}$       set of control points
3:    $t$                                 real number
4: Output
5:    $P_0^{(n)} = B_P(t)$               the point on the Beziér curve w.r.t. to  $t$ 
6: procedure DECASTELJAU( $P, t$ )
7:    $P^{(0)} \leftarrow P$ 
8:   for  $j = 1, 2, \dots, n$  do
9:     for  $k = 0, 1, \dots, n - j$  do
10:       $P_k^{(j)} \leftarrow (1 - t) \cdot P_k^{(j-1)} + t \cdot P_{k+1}^{(j-1)}$ 
   return  $P_0^{(n)}$ 

```

Theorem 2.1.3. Algorithm 1 computes $B_P(t)$.

Proof. By induction. Let $n = 1$. Then

$$P_0^{(1)} = (1 - t) \cdot P_0 + t \cdot P_1.$$

By employing the induction hypothesis

$$P_j^{(n)} = \sum_{k=j}^{n+j} \binom{n}{k} (1-t)^{n-k} t^k P_{j+k}$$

for some $n \in \mathbb{N}$, we can infer that

$$\begin{aligned}
P_0^{(n+1)} &= (1-t) \cdot P_0^{(n)} + t \cdot P_1^{(n)} \\
&= (1-t) \cdot \sum_{k=0}^n \binom{n}{k} (1-t)^{n-k} t^k P_k + t \cdot \sum_{k=1}^{n+1} \binom{n}{k} (1-t)^{n-k} t^k P_{k+1} \\
&= \sum_{k=0}^{n+1} \binom{n+1}{k} (1-t)^{n+1-k} t^k P_k,
\end{aligned}$$

which is equal to $B_P(t)$ for degree $n+1$. \square

A visual representation of Algorithm 1 yields a triangular scheme. To compute one point on a Beziér curve B_P with degree n , one has to perform $\frac{n^2-n}{2}$ vector additions and $n^2 - n$ scalar multiplications.

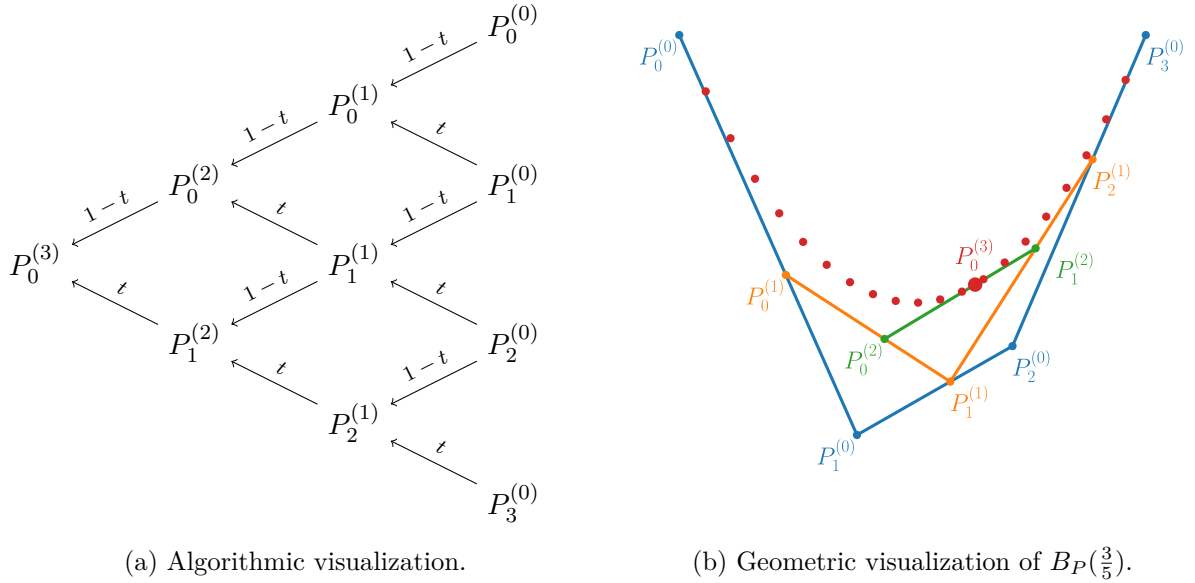


Figure 2.2: Visual representations of de Casteljau's algorithm.

Interestingly, the representation of the algorithm in Figure 2.2 also gives rise to an intuitive visualization of the geometric shape of the Beziér curve B_P . For all $i \in \{0, \dots, n\}$ and all $j \in \{0, \dots, n-i\}$, the point $P_j^{(i+1)}$ is the convex combination (always w.r.t. t) of $P_j^{(i)}$ and $P_{j+1}^{(i)}$. Thus $P_j^{(i+1)}$ always lies on the line segment between $P_j^{(i)}$ and $P_{j+1}^{(i)}$, as can be observed in the example in Figure 2.2.

2.1.3 Properties

Other than being remarkably intuitive, Beziér curves have a lot of properties which make them convenient. In computer-aided design software, most graphical user interfaces rely on the principle of letting the user interactively drag and drop the control points with a mouse, granting them control over the shape of Beziér curve. The following theorems further illustrate why this is a good idea.

Theorem 2.1.4. $B_P(0) = P_0$ and $B_P(1) = P_n$.

Proof. Explicit computation yields

$$B_P(0) = \sum_{k=0}^n \binom{n}{k} t^k P_k = \binom{n}{0} P_0 = P_0$$

and

$$B_P(1) = \sum_{k=0}^n \binom{n}{k} (1-t)^{n-k} P_k = \binom{n}{n} P_n = P_n.$$

□

Theorem 2.1.5. Let $T \in \mathbb{R}^{3 \times 3}$. Then $B_{TP}(t) = TB_P(t)$ where $TP := \{TP_0, TP_1, \dots, TP_n\}$.

Proof. For all $t \in [0, 1]$ we can directly compute

$$TB_P(t) = \sum_{k=0}^n \binom{n}{k} (1-t)^{n-k} t^k TP_k = B_{TP}(t).$$

□

Theorem 2.1.6. $B_P(t)$ lies in the convex hull of P for all $t \in [0, 1]$.

Proof. By the algorithm of de Casteljau (1), we know that $P_j^{(i)} = (1-t) \cdot P_j^{(i-1)} + t \cdot P_{j+1}^{(i-1)}$ for all $t \in [0, 1]$. Therefore, $P^{(i)}$ lie in the convex hull of $P^{(i-1)}$. But then $B_P(t) = P_0^{(n)}$ always lies in the convex hull of $P^{(0)} = P$ by induction. □

Simple as their appearance may be, Beziér curves fall short of representing some of the most common geometric shapes. Given a finite number of control points, we can never make $B_P(t)$ a circular arc, although a circle has a very simple parametric form. One of their greatest perks, the ability to describe a shape with just a handful of control points, is their greatest shortcoming at the same time. This is most likely the reason why Beziér curves are not the state of the art in technical engineering applications. However, Beziér curves certainly do provide an intuition for Non-Uniform Rational B-Splines or NURBS, which is their prevailing counterpart.

2.2 Non-Uniform Rational B-splines (NURBS)

NURBS are a state of the art tool for curve and surface modelling. There is a somewhat common joke that describes the acronym NURBS as "*Nobody Understands Rational B-Splines*" (source?). In this section, we invalidate this punch line. First of all, we discuss B-splines, then we construct B-spline curves and surfaces and then we apply simple transformations to the B-spline curves and surfaces to acquire NURBS curves and surfaces.

2.2.1 Definition

Similarly to how Beziér curves are defined on the Bernstein polynomial basis, NURBS are defined on basis functions called basis splines or, more commonly, B-splines.

Definition 2.2.1. A *knot sequence* $(t_m)_{m=-\infty}^{\infty} \subset \mathbb{R}$ is a sequence with $t_m \leq t_{m+1}$ for all $m \in \mathbb{Z}$.

Definition 2.2.2. The *B-splines of degree 0* on a knot sequence (t_m) are defined as

$$N_{1,k}^{(t_m)}(t) := \begin{cases} 1 & \text{if } t \in [t_k, t_{k+1}), \\ 0 & \text{else.} \end{cases} \quad (2.5)$$

The *B-splines of degree $p - 1$* with $p > 1$ are given by the *Cox-de-Boor recursion formula*

$$N_{p,k}^{(t_m)}(t) := \omega_{p-1,k}^{(t_m)}(t) N_{p-1,k}^{(t_m)}(t) + (1 - \omega_{p-1,k+1}^{(t_m)}(t)) N_{p-1,k+1}^{(t_m)}(t), \quad (2.6)$$

where

$$\omega_{p,k}^{(t_m)}(t) := \begin{cases} \frac{t - t_k}{t_{k+p} - t_k} & \text{if } t_{k+p} \neq t, \\ 0 & \text{else.} \end{cases} \quad (2.7)$$

Remark. Instead of $N_{p,k}^{(t_m)}$ we write $N_{p,k}$ and explicitly refer to (t_m) when necessary. We restrict the domain of definition of $N_{p,k}$ to $[0, 1]$ by setting $\lim_{m \rightarrow -\infty} t_m = 0$ and $\lim_{m \rightarrow \infty} t_m = 1$.

Definition 2.2.3. Let V a vector space. A *B-spline curve* of degree $p - 1$ over a set of control points $P = \{P_0, P_1, \dots, P_n\} \subset V$ and a knot sequence (t_m) is defined as

$$S_P(t) = \sum_{k=0}^n N_{p,k}(t) P_k.$$

Definition 2.2.4. A *NURBS curve* $C_P(t)$ of degree $p - 1$ with the control points $P = \{P_0, P_1, \dots, P_n\} \subset V$, the control weights $w = (w_0, w_1, \dots, w_n) \subset \mathbb{R}$ and a knot sequence (t_m) is defined as

$$C_P(t) = \frac{\sum_{k=0}^n N_{p,k}(t) w_k P_k}{\sum_{k=0}^n N_{p,k}(t) w_k}. \quad (2.8)$$

Remark. Let $\dim V = d$. A NURBS curve can alternatively be understood as a projection of a B-spline curve on a transformed set of control points. For this purpose we define the embedding into the weighted vector space

$$\Phi_w : V \rightarrow V \times \mathbb{R}$$

that maps each control point $P_k = (p_1, \dots, p_d) \in V$ onto $(w_k p_1, \dots, w_k p_d, w_k) \in V \times \mathbb{R}$. We also have to define the projection map

$$\Phi^\dagger : V \times \mathbb{R} \rightarrow V$$

that maps each point on the B-spline curve $S_{\Phi(P)}(t) = (s_1, \dots, s_d, s_{d+1})$ onto $(\frac{s_1}{s_{d+1}}, \dots, \frac{s_d}{s_{d+1}})$. We can then define the NURBS curve as

$$C_P(t) = \Phi^\dagger(S_{\Phi_w(P)}(t))$$

which we will make use of later on.

Theorem 2.2.5. Let $w \equiv 1$. Then $S_P \equiv \Phi^\dagger(S_{\Phi_w(P)})$. In other words, NURBS curves are a generalization of B-spline curves.

Proof. Since in this case $\Phi_w((p_1, \dots, p_d)) = (p_1, \dots, p_d, 1)$, we have that $\Phi^\dagger(S_{\Phi_w(P)}(t)) = \Phi^\dagger(\Phi_w(S_P(t))) = S_P(t)$. \square

Now that we have defined B-spline curves and NURBS curves, we can define B-spline surfaces and NURBS surfaces in a similar manner. To do this, we require a grid of knots represented by two knot sequences $(u_m)_{m=-\infty}^\infty$ and $(v_m)_{m=-\infty}^\infty$ which satisfy the same conditions as (t_m) did before. Instead of a one-dimensional set of control points, the surface definition relies on a two-dimensional set of control points. Notice that this grants us control

Definition 2.2.6. A *B-spline surface* $S_P(u, v)$ of degree $(p-1, q-1)$ over a set of control points $P = \{P_{i,j} : (i, j) \in \{0, 1, \dots, n_u\} \times \{0, 1, \dots, n_v\}\} \subset V$ on the knot grid $(u_m), (v_m)$ is defined as

$$S_P(u, v) = \sum_{k_u=0}^{n_u} \sum_{k_v=0}^{n_v} N_{p,k_u}(u) N_{q,k_v}(v) P_{k_u,k_v},$$

where $N_{p,k_u}(u) := N_{p,k_u}^{(u_m)}(u)$ and $N_{q,k_v}(v) := N_{q,k_v}^{(v_m)}(v)$.

Definition 2.2.7. A *NURBS surface* $C_P(u, v)$ of degree $(p-1, q-1)$ over a set of control points $P = \{P_{i,j} : (i, j) \in \{0, 1, \dots, n_u\} \times \{0, 1, \dots, n_v\}\} \subset V$, the control weights $w = \{w_{i,j} : (i, j) \in \{0, 1, \dots, n_u\} \times \{0, 1, \dots, n_v\}\} \subset \mathbb{R}$ and the knot grid $(u_m), (v_m)$ is defined as

$$C_P(u, v) = \frac{\sum_{k_u=0}^{n_u} \sum_{k_v=0}^{n_v} N_{p,k_u}(u) N_{q,k_v}(v) w_{k_u,k_v} P_{k_u,k_v}}{\sum_{k_u=0}^{n_u} \sum_{k_v=0}^{n_v} N_{p,k_u}(u) N_{q,k_v}(v) w_{k_u,k_v}},$$

where $N_{p,k_u}(u) := N_{p,k_u}^{(u_m)}(u)$ and $N_{q,k_v}(v) := N_{q,k_v}^{(v_m)}(v)$.

Remark. As with NURBS curve, we have the analogous result

$$C_P(u, v) = \Phi^\dagger(S_{\Phi_w(P)}(u, v))$$

for NURBS surfaces.

The notion of the knot sequence (t_m) is commonly computationally simplified to that of a knot vector τ , since τ only contains a finite number of elements. For our purposes, we let

$$\tau = (\underbrace{t_0, \dots, t_{p-1}}_{=0}, t_p, \dots, t_n, \underbrace{t_{n+1}, \dots, t_{n+p}}_{=1}),$$

where $t_k = 0$ for $k \in \{0, \dots, p-1\}$ and $t_k = 1$ for $k \in \{n+1, \dots, n+p\}$. We still require the monotony property $t_k \leq t_{k+1}$ for all $k \in \{0, \dots, n+p\}$.

2.2.2 De Boor's Algorithm

To efficiently calculate points on a B-spline object, Carl-Wilhelm Reinhold de Boor devised an efficient algorithm, the construction of which demonstrates its correctness. Together with the embedding Φ_w and the projection Φ^\dagger from the Remark for Definition 2.2.4, this algorithm can also be used to calculate points on a NURBS object.

Let $P = \{P_0, P_1, \dots, P_n\}$ a set of control points, (t_m) a knot sequence and $p - 1$ the degree of the B-spline curve $S(t)$. Then by the Cox-de-Boor recursion formula, we find

$$\begin{aligned} S(t) &= \sum_{k=0}^n N_{p,k}(t) P_k \\ &= \sum_{k=1}^n \omega_{p-1,k}(t) N_{p-1,k}(t) P_k + \sum_{k=0}^n (1 - \omega_{p-1,k+1}(t)) N_{p-1,k+1}(t) P_k. \end{aligned}$$

Changing the limits of the second term, we can summarize the two terms as

$$\begin{aligned} S(t) &= \sum_{k=1}^n N_{p-1,k}(t) \underbrace{\left[\omega_{p-1,k}(t) P_k + (1 - \omega_{p-1,k}(t)) P_{k-1} \right]}_{=: P_k^{(1)}(t)} \\ &= \sum_{k=1}^n N_{p-1,k}(t) P_k^{(1)}(t). \end{aligned}$$

Recursively defining

$$P_k^{(j)}(t) := \begin{cases} \omega_{p-j,k} P_k^{(j-1)}(t) + (1 - \omega_{p-j,k}) P_{k-1}^{(j-1)}(t) & \text{if } j > 0, \\ P_k & \text{else,} \end{cases} \quad (2.9)$$

we can repeat this process up to $p - 2$ more times, finding

$$S(t) = \sum_{k=p-1}^n N_{1,k}(t) P_k^{(p-1)}(t) = P_l^{(p-1)}(t)$$

for $t \in [t_l, t_{l+1})$. We can thus use the recursive definition in Equation 2.9 as the key step of our algorithm to compute $S(t)$. It is already clear from this place that the points calculated on a B-spline curve are in fact also a cumulated convex combination of control points, just as it is the case with Beziér curves. As zero-values for $\omega_{i,j}$ (or $1 - \omega_{i,j}$) can be completely omitted by checking multiplicity, we arrive at the following algorithm:

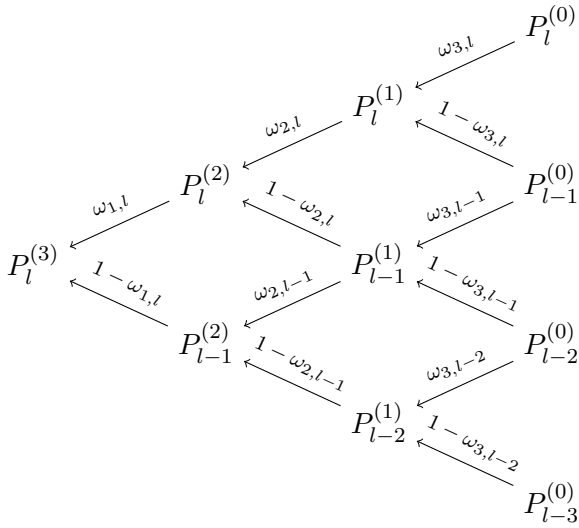
Algorithm 2 de Boor's algorithm for curves

```

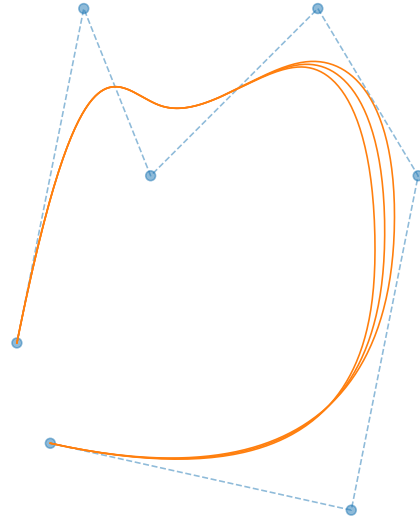
1: Input
2:    $P = \{P_0, P_1, \dots, P_n\}$       set of control points of the B-spline curve
3:    $\tau = (t_0, t_1, \dots, t_{n+p})$     knot vector of the B-spline curve
4:    $p - 1$                             degree of the B-spline curve
5:    $t \in [t_0, t_{n+p})$               real number

6: Output
7:    $S_P(t)$                           the point on the B-spline curve w.r.t. to  $t$ 

8: procedure DEBOORCURVE( $P, p, \tau, t$ )
9:   Find  $l$  such that  $t \in [t_l, t_{l+1})$ 
10:  Let  $m$  be the multiplicity of  $t$  in the knot vector  $\tau$ 
11:   $P^{(0)} \leftarrow P$ 
12:  for  $j = 1, 2, \dots, p - m - 1$  do
13:    for  $k = l - p + j + 1, \dots, l - m$  do
14:       $\omega_{p-j,k} \leftarrow \frac{t - t_k}{t_{k+p-j} - t_k}$ 
15:       $P_k^{(j)} \leftarrow (1 - \omega_{p-j,k}) \cdot P_{k-1}^{(j-1)} + \omega_{p-j,k} \cdot P_k^{(j-1)}$ 
16:  return  $P_{l-m}^{(p-m-1)} = C_P(t)$ 
  
```



(a) Visualization of de Boor's algorithm on a curve $S_P(t)$ with degree 3, where t does not appear in the knot vector τ (in other words, $m = 0$).



(b) Degree 3 NURBS curve $\Phi^\dagger(S_{\Phi_w(P)}(t))$ for different values of a single entry of the control weight vector w .

Figure 2.3: Calculating points on a NURBS curve.

To calculate one point on the B-spline curve S_P of degree p , we require at most $\frac{p^2-p}{2}$ vector additions and $p^2 - p$ scalar multiplications, which is quite similar to what we found for Bézier curves. However, we also need to calculate $\omega_{j,k}$ at every step, which in total sums up to $p^2 - p$ real additions and $\frac{p^2-p}{2}$ real multiplications.

By writing the definition of the B-spline surface as

$$S_P(u, v) = \sum_{k_u=0}^{n_u} \sum_{k_v=0}^{n_v} N_{p,k_u}(u) N_{q,k_v}(v) P_{k_u,k_v} = \sum_{k_u=0}^{n_u} N_{p,k_u}(u) \underbrace{\left(\sum_{k_v=0}^{n_v} N_{q,k_v}(v) P_{k_u,k_v} \right)}_{:= q_{k_u}(v)},$$

we can observe that Algorithm 2 can be utilized to calculate points on B-splines surfaces. To do this, we run the de Boor's algorithm to calculate $q_{k_u}(v)$.

Algorithm 3 de Boor's algorithm for surfaces

```

1: Input
2:    $P = \{P_{i,j}\}$            set of control points with  $n_1 \cdot n_2$  elements
3:    $\tau_u = (u_0, u_1, \dots, u_{n_u+p})$    first knot vector of the B-spline curve
4:    $\tau_v = (v_0, v_1, \dots, v_{n_v+q})$    second knot vector of the B-spline curve
5:    $p - 1$                    first degree of the B-spline curve
6:    $q - 1$                    second degree of the B-spline curve
7:    $u \in [u_0, u_{n_u+p})$        first real number
8:    $v \in [v_0, v_{n_v+q})$        second real number

9: Output
10:   $S_P(u, v)$                the point on the B-spline curve w.r.t. to  $u, v$ 

11: procedure DEBOORSURFACE( $P, p, q, \tau_u, \tau_v, u, v$ )
12:   Find  $l$  such that  $u \in [u_l, u_{l+1})$ 
13:   Let  $m$  be the multiplicity of  $u$  in the knot vector  $\tau_u$ 
14:   for  $k = l - p + 1, \dots, l - m - 1$  do
15:      $Q_k \leftarrow \text{deBoorCurve}(P_{k,\cdot}, q, \tau_v, v)$ 
   return  $\text{deBoorCurve}(Q, p, \tau_u, u)$ 

```

Utilizing the notation with the embedding map Φ_w and the projection map Φ^\dagger , we can calculate points on NURBS objects with these two algorithms. To do this, we employ the following steps on a set of control points P and the weights w :

1. Calculate $P_w = \Phi_w(P)$.
2. Use de Boor's algorithm to calculate points on S_{P_w} .
3. Project points onto V by applying Φ^\dagger to S_{P_w} to find C_P .

2.2.3 Properties

In this section, we will see that B-spline curves and NURBS curves share some (although not all) useful properties with Beziér curves.

Theorem 2.2.8. Let S_P a B-spline curve and C_P a NURBS curve. Then $S_P(0) = P_0$ and $S_P(1) = P_n$ and therefore $C_P(0) = P_0$ and $C_P(1) = P_n$.

Proof. By using Algorithm 2, we have $m = p$ and return P_l without calculation, which is P_0 in the case of $t = 0$ and P_n in the case of $t = 1$. Then by $C_P(t) = \Phi^\dagger(S_{\Phi_w(P)}(t))$, we have $C_P(0) = \Phi^\dagger\Phi_w(P_0) = P_0$ and $C_P(1) = \Phi^\dagger\Phi_w(P_n) = P_n$. \square

Theorem 2.2.9. Let $V = \mathbb{R}^d$ and $T \in \mathbb{R}^{d \times d}$. Let S_P be a B-spline curve or surface and C_P a NURBS curve or surface. Then $S_{TP} = TS_P$ and $C_{TP} = TC_P$.

Proof. By linearity of T we can compute

$$S_{TP}(t) = \sum_{k=0}^n N_{p,k}(t)TP_k = T \left(\sum_{k=0}^n N_{p,k}(t)P_k \right) = TS_P(t)$$

for B-spline curves and

$$C_{TP}(t) = \frac{\sum_{k=0}^n N_{p,k}(t)w_kTP_k}{\sum_{k=0}^n N_{p,k}(t)w_k} = T \left(\frac{\sum_{k=0}^n N_{p,k}(t)w_kP_k}{\sum_{k=0}^n N_{p,k}(t)w_k} \right) = TC_P(t)$$

for NURBS curves. Similarly, we can compute

$$S_{TP}(u, v) = \sum_{k_u=0}^{n_u} \sum_{k_v=0}^{n_v} N_{p,k_u}(u)N_{q,k_v}(v)TP_{k_u,k_v} = TS_P(u, v)$$

for B-spline surfaces and

$$C_{TP}(u, v) = \frac{\sum_{k_u=0}^{n_u} \sum_{k_v=0}^{n_v} N_{p,k_u}(u)N_{q,k_v}(v)w_{k_u,k_v}TP_{k_u,k_v}}{\sum_{k_u=0}^{n_u} \sum_{k_v=0}^{n_v} N_{p,k_u}(u)N_{q,k_v}(v)w_{k_u,k_v}} = TC_P(u, v)$$

for NURBS surfaces. \square

Theorem 2.2.10. A B-spline curve or surface S_P lies in the convex hull of its control points P .

Proof. Using Equation 2.9, we can see that every iteration of Algorithm 2 produces a set of points which all lie in the convex hull of the last iteration. Therefore, $S_P(t) = P_l^{(p-1)}$ lies in the convex hull of $P^{(0)}$ for all l . \square

Remark. This theorem does not hold for NURBS curves and surfaces C_P .

2.3 Methods on NURBS Objects

2.3.1 Point Inversion

Let $\gamma(t) \subset \mathbb{R}^d$ a curve, $t \in [0, 1]$, and let $Q \in \mathbb{R}^d$ a point. We want to find

$$t^* = \arg \min_{t \in [0, 1]} D(\gamma(t), Q),$$

where $D(\cdot, \cdot)$ is the Euclidean distance between two points. Notice that

$$\min_{t \in [0, 1]} D(\gamma(t), Q) = D(\gamma(t^*), Q)$$

is the distance between the curve γ and the point Q .

Definition 2.3.1. The distance between a curve $\gamma \subset \mathbb{R}^d$ and a point $Q \in \mathbb{R}^d$ is given by

$$D(Q, \gamma) := D(\gamma, Q) := \min_t D(\gamma(t), Q).$$

Minimizing distance functions is, in general, a problem that is hard to solve. We therefore make some assumptions about the point-curve distance function $\phi(t) := D(\gamma(t), Q)$ that we are going to minimize in order to find the target parameter t^* . If ϕ is convex and differentiable, then the problem statement has a well-known and easy to implement solution, namely Newton's method, which for an initial guess $t^{(0)}$ is given by the iteration

$$t^{(n+1)} = t^{(n)} - \frac{\phi(t^{(n)})}{\phi'(t^{(n)})}.$$

Here, $\phi'(t)$ is the derivative of $\phi(t)$ with respect to t , which for a small value of $\epsilon > 0$ can be approximated by the right-sided difference quotient

$$\phi'_r(t) = \frac{\phi(t + \epsilon) - \phi(t)}{\epsilon}.$$

However, to ensure differentiability of ϕ adjacent to t , it is recommended to compare the value of the right-sided difference quotient to

$$\phi'_l(t) = \frac{\phi(t) - \phi(t - \epsilon)}{\epsilon},$$

which is the left-sided difference-quotient. If $\phi'_r(t) = \phi'_l(t)$, then we can assume $\phi'_l(t) \approx \phi'(t) \approx \phi'_r(t)$.

Although in CoolingGen, we often cannot make the assumption of differentiability or convexity of ϕ . We therefore employ a pragmatic scheme and assume continuity, piecewise differentiability and piecewise convexity of ϕ and run Newton's method on a small subinterval $[l, u] \subset [0, 1]$.

To find $[l, u]$, we sample the curve γ at a set of points $\{t_0, t_1, \dots, t_n\}$ with $t_i = i/n$ and seek

$$m = \arg \min_{t \in \{t_0, t_1, \dots, t_n\}} \phi(t).$$

We let $l = m - \frac{i}{n}$ and $u = m + \frac{i}{n}$. Next, we can use Newton's method with the start value m to find

$$t^* = \arg \min_{t \in [l, u]} \phi(t).$$

This scheme will only converge to the global minimum of ϕ for large enough $n \in \mathbb{N}$.

Notice that if $\phi(t^*) = 0$, we have that the intersection of the curve γ with the point Q is equal to Q . In other words, the point Q intersects the curve γ . Given that γ is a NURBS curve, we can then observe that the devised algorithm is the inversion of de Boor's algorithm (Algorithm 2), that will return the input parameter of the curve that fits the point Q . This justifies the name *point inversion algorithm*.

Notice also that t^* is not necessarily unique, as multiple points on a curve γ can share the same minimum distance to a given point Q . However, we are happy to find one such point in our applications, as most of the time, the point of interest is going to fulfill $\phi(t^*) = 0$. Assume there is another value $s^* \neq t^*$ that has minimum distance to Q . Then $\phi(s^*) = \phi(t^*) = 0$. But then because both of those values return exactly 0 and because of the point-separating property of the Euclidean norm, our point of interest Q lies on the curve *twice*, in the sense that the map γ is not injective at that point. But that means γ has a self intersection at $\gamma(t^*) = \gamma(s^*)$. So if we assume injectivity of γ and only seek the parameters of points Q that lie inside of γ , we do not have to worry about this matter any more.

To summarize, the algorithm can be described in pseudo-code

Algorithm 4 Point Inversion

```

1: Input
2:    $\gamma, Q$                 curve and point
3:    $N$                     number of samples for initial value search
4:    $M$                     number of iterations in Newton's method
5: Output
6:    $t^*$                   best parameter of  $\gamma$ 
7: procedure FINDPOINTINVERSIONINITVALUES( $\gamma, Q$ )
8:    $m \leftarrow 0$ 
9:   for  $k = 1, \dots, N$  do
10:     $t \leftarrow \frac{k}{N}$ 
11:    if  $D(Q, \gamma(m)) > D(Q, \gamma(t))$  then  $m \leftarrow t$ 
12:    return  $m - \frac{i}{N}, m + \frac{i}{N}, m$ 
13: procedure POINTINVERSION( $\gamma, Q$ )
14:    $l, u, m \leftarrow \text{findPointInversionInitValues}(\gamma, Q)$ 
15:    $t_0 \leftarrow m$ 
16:   for  $k = 1, 2, \dots, M$  do
17:     $t_1 \leftarrow t_0 + \epsilon$ 
18:     $\phi_0 \leftarrow D(\gamma(t_0), Q)$  and  $\phi_1 \leftarrow D(\gamma(t_1), Q)$ 
19:     $\phi' \leftarrow \frac{\phi_1 - \phi_0}{\epsilon}$ 
20:     $t_0 \leftarrow t_0 - \frac{\phi_0}{\phi'}$ 
21:    if  $t_0 < l$  then  $t_0 \leftarrow l$ 
22:    if  $t_0 > u$  then  $t_0 \leftarrow u$ 
23:   return  $t_0$ 

```

2.3.2 Ray-Curve Intersection

Definition 2.3.2. A ray with support vector $A \in V$ and direction vector $B \in V$ is given by the set of points

$$\{A + tB : t \in \mathbb{R}, t \geq 0\}. \quad (2.10)$$

The dependence of a point on the ray on the real parameter t motivates the description of this set as a map

$$R_{A,B} : \mathbb{R} \rightarrow V, \quad t \mapsto A + tB.$$

where Equation 2.10 is then equal to $R_{A,B}([0, \infty))$.

In this section, we want to find an algorithm that intersects a curve $\gamma(t)$ with $t \in [0, 1]$ with a ray $R_{A,B}(s)$ with $s \in [0, \infty)$. Generally, the intersection of these two sets can be written as

$$I = \gamma([0, 1]) \cap R_{A,B}([0, \infty)).$$

The algorithm presented will return only up to one element in that set, specifically the one corresponding to the lowest value of the ray parameter s . If however $I = \emptyset$, then no element will be returned.

Definition 2.3.3. Let $R_{A,B}$ a ray and $\gamma(t)$ a curve. Then the ray-curve-distance w.r.t $R_{A,B}$ and γ is defined as

$$D(R_{A,B}, \gamma) := D(\gamma, R_{A,B}) := \min_{s \in [0, \infty)} D(\gamma, R_{A,B}(s))$$

Definition 2.3.4. Let $R_{A,B}(s)$ a ray and $\gamma(t)$ a curve. If a solution to

$$\min_{s \in [0, \infty)} s \quad \text{subject to} \quad D(\gamma, R_{A,B}) = 0$$

exists, then it is called *collision parameter* of $R_{A,B}$ w.r.t. γ .

We define the return value of our algorithm as the one element set given by

$$I_{\min} := \begin{cases} \{R_{A,B}(s^*)\} & \text{if } D(R_{A,B}(s^*), \gamma) \leq \epsilon, \\ \emptyset & \text{otherwise,} \end{cases}$$

where the absolute tolerance $\epsilon > 0$ is close to 0 and s^* is an approximation of the collision parameter of $R_{A,B}$ w.r.t. γ . If $I_{\min} \neq \emptyset$, then we refer to the element in I_{\min} as *collision point*.

Remark. Why is the notion of the collision point of interest? To exemplify the prospect of our algorithm, imagine the following scenario: Let there be a reflective interface represented by a curve γ and a beam of light represented by a ray $R_{A,B}$. Then our model suggests the equivalence of the physical point of reflection and the collision point of the ray with respect to the curve.

We can find the approximation s^* of the collision parameter by using a common CAD scheme called *ray marching*, in which we traverse the ray $R_{A,B}$ by a small distance increments s until we achieve collision with the curve γ . How do we choose the optimal value for s ? The idea is the following: Using the point inversion algorithm, we can calculate the *safe distance* s of the point A on the ray to the curve γ . Then we can easily construct a point P that fulfills $D(A, P) = s$ and lies on the ray $R_{A,B}$ by

$$P := A + s \frac{B}{\|B\|}.$$

Now there are only two possibilities: Either P lies within the ϵ -ball of the collision point, or the line segment $\overline{AP} \subset R_{A,B}([0, \infty))$ does not intersect with γ . In the first case, we can happily return $\{P\}$. In the second case, we can repeat the procedure on the set

$$R_{A,B}([0, \infty)) \setminus \overline{AP} = R_{A,B}([s, \infty)) = R_{P,B}([0, \infty)).$$

If after a certain amount of iterations N the algorithm does not converge to a point which lies within the ϵ -ball of the collision point, we return \emptyset .

Algorithm 5 Ray Marching

```

1: Input
2:    $\gamma$                                 curve
3:    $R_{A,B}$                              ray
4: Output
5:    $I_{\min}$                             intersection set with up to one element
6: procedure INTERSECTCURVERAY( $\gamma, A, B$ )
7:    $B \leftarrow \frac{B}{\|B\|}, s \leftarrow 0, P \leftarrow A$ 
8:   for  $k = 1, 2, \dots, N$  do
9:      $s \leftarrow s + D(\gamma(\text{pointInversion}(\gamma, P)), P)$ 
10:     $P \leftarrow A + sB$ 
11:    if  $s < \epsilon$  then return  $\{P\}$ 
return  $\emptyset$ 

```

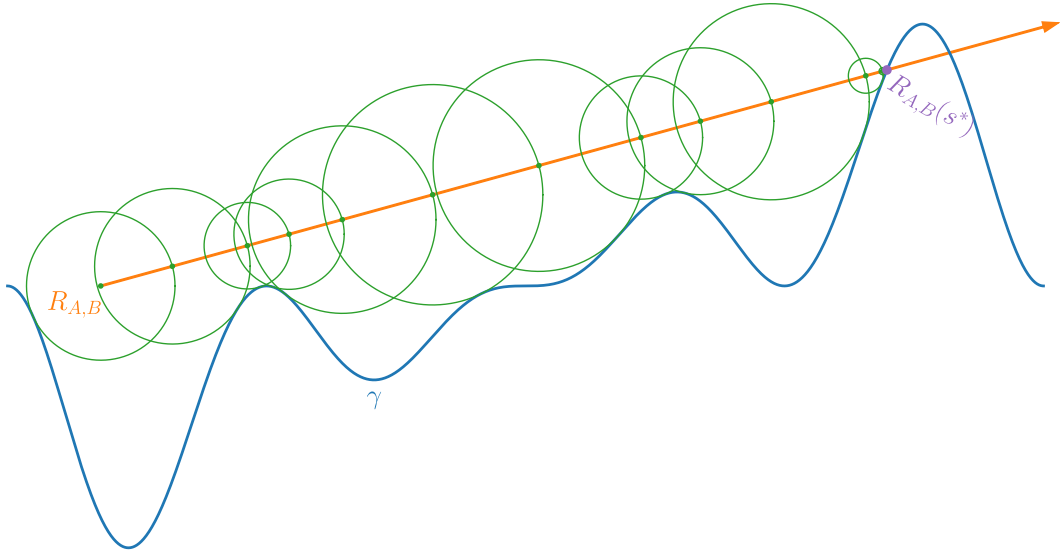


Figure 2.4: The ray marching algorithm visualized: At each iteration, a new safe distance s (depicted as green circle radii) along the ray is calculated. The ray is traversed using s as step size (to achieve the points depicted in green) until the safe distance falls below the absolute tolerance ϵ . The resulting point is close to the collision point depicted in purple.

2.3.3 Curve-Curve Intersection

2.3.4 Fillet Creation

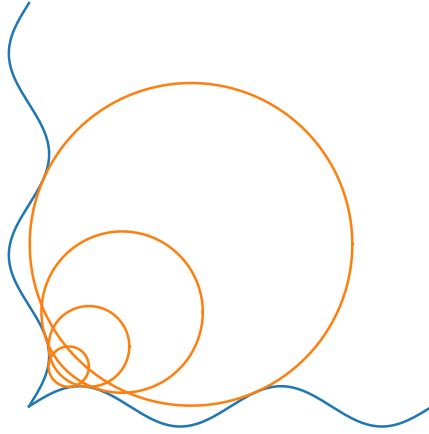


Figure 2.5: yeah

2.4 Jet Engine Design Specifics

2.4.1 Fundamental Terms

2.4.2 The S2M Net

3 Results

3.1 Cooling Geometries And Their Parametrizations

3.1.1 Chambers

3.1.2 Turnarounds

3.1.3 Slots

3.1.4 Film Cooling Holes

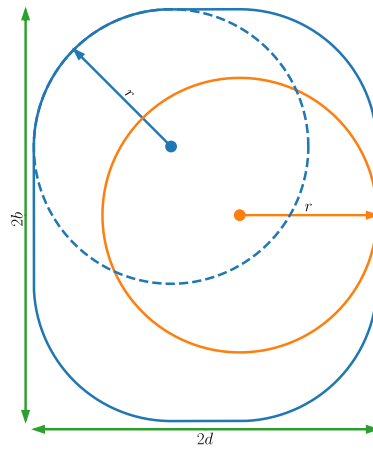


Figure 3.1: yeah

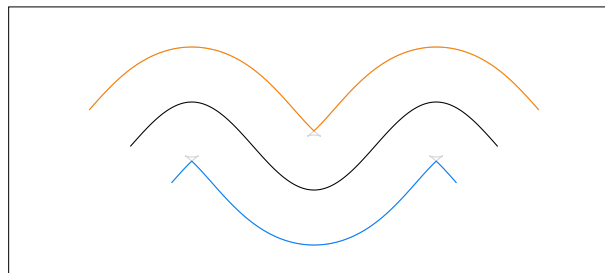


Figure 3.2: yeah

3.1.5 Impingement Inserts

3.2 Export for CENTAUR

3.3 Export for Open CASCADE

4 Discussion

4.1 Future Work

4.2 Conclusion

[Pie97]

5 References

- [Béz68] Pierre E. Bézier. “How Renault Uses Numerical Control for Car Body Design and Tooling”. In: *SAE Technical Paper Series*. SAE International, Feb. 1968. DOI: 10 . 4271/680010.
- [Pie97] Les A. Piegl. *The NURBS book*. Springer, 1997, p. 646. ISBN: 3540615458.